Hindawi
Shock and Vibration
Volume 2021, Article ID 5579967, 14 pages
https://doi.org/10.1155/2021/5579967

Research Article

Study on Key Parameters of Directional Long Borehole Layout in High-Gas Working Face

Zhenguo Yan,[1] **Yanping Wang**,[1] **Jingdao Fan**,[1,2,3] **Yuxin Huang**,[1] **and Yanpeng He**[4]

[1]*School of Safety Science and Engineering, Xi'an University of Science and Technology, Shaanxi, Xi'an 710054, China*
[2]*Shananxi Yanchang Petroleum(Group) Co., LTD., Xi'an 710075, China*
[3]*Innovation Center of Intelligent Mining Technology in Coal Mine, Ministry of Emergency Management of the People's Republic of China, Huangling 727307, China*
[4]*School of Energy Engineering, Xi'an University of Science and Technology, Shaanxi, Xi'an 710054, China*

Correspondence should be addressed to Zhenguo Yan; yanzhenguo@xust.edu.cn

Received 10 February 2021; Revised 27 February 2021; Accepted 8 March 2021; Published 30 March 2021

Academic Editor: Feng Du

This research aims to obtain a new way based on the directional long borehole layout to investigate the gas migration behavior of coal bed methane. In view of the study of the oil-type gas reservoir and the influence range of mining on the working face in the surrounding rock, the paper puts forward the optimization method of the directional long borehole layout of the surrounding rock and the method of the borehole layout with comprehensive consideration of the influence of mining on the failure of the roof and floor and the distribution of surrounding rock gas-bearing reservoirs. The test results showed that the layout horizon of the directional long boreholes is determined, and the layout was within the height range of 20–40 meters, clarified the relationship between the drainage data and the exposure level of the borehole and the layout of the borehole, compared the gas concentration in the upper corner of the working face before and after the drainage, and constructed a three-dimensional comprehensive drainage mode for the high-gassy working face, which provided a worth-promoting method that supports surrounding rock oil-type gas and gas treatment in the high-gas mining area.

1. Introduction

China is one of the countries with the most serious coal mine gas problem in the world, and gas disaster is the biggest threat to coal mine safety production. It has been proved that gas extraction is the fundamental measure to prevent and control coal mine gas disasters and accidents. With gas extraction, gas accidents in the process of coal mining, such as gas overshoot, gas explosion, and coal and gas outbursts, can be effectively solved. By doing so, the safe production of the coal mine can be guaranteed. However, the existing gas control technology is mainly to solve the gas extraction. To realize three-dimensional comprehensive gas extraction technology with full space coverage, it is necessary to carry out "preproduction gas extraction, in-production gas extraction, and pressure-relief gas extraction" simultaneously. The key problem is to control the borehole trajectory accurately, which is the directional drilling technology of the surrounding rock.

High-gas mines and outburst mines contribute to more than 30% of the coal production capacity in China. In view of this, coordinating the development and use of coal and gas has become an urgent concern for China's coal industry. Wang et al. [1] and Jiang et al. [2] researched the influence of the long borehole when it comes to coal and coal-bed methane extraction based on the example of coal mines in China's mining area. With the increase mining depth of coal mines in China, the quantity of outburst mines and outburst coal seams keeps increasing; Cheng and Yu [3,4] expatiated the necessity of controlling gas in the long drilling hole. Bai et al. [5] and Wang et al. [6] analyzed the influence of different methods on gas adsorption analysis, such as longhole directional drilling technology.

In addition, Liu et al. [7] provided the Jincheng mode based on directional long borehole coal mining. Chae et al. [8] and Zhou and Yan [9] studied the influence of borehole size to the gas flow. Yang et al. [10] established a simplified ROP model for soft coal seams to improve drilling efficiency. The results of Shakib et al. [11] can be used to support the improved directional drilling system design. Jiang and Miao [12] analyzed the necessity and feasibility of the kilometer drill test in the Jinmei Group and its application prospect in gas development and control.

To further improve the application of directional long drilling construction technology in the coal seam surrounding rock, efficient preextraction of coal seam gas and surrounding rock oil-type gas can effectively prevent the problem of gas concentration exceeding the limit in the upper corner of goaf. At the same time, the prepumping drilling can be used for both geological exploration and "one hole for multiple purposes." The layer of the directional long hole in the surrounding rock was selected specifically, and the implementation effect of the directional long hole was tested, so as to provide practical reference for replacing the roadway with holes and provide the development direction for the technical breakthrough of traditional roof high-position hole technology.

2. Test Conditions and Methods

2.1. Geological Condition of the Test Working Face. Huangling No. 2 coal mine is located in Huangling County, Shaanxi Province. The geographical coordinates are as follows: east longitude 108°45′06″~108°58′34″ and north latitude 35°30′30″~35°48′06″. The mine area is about 352 km^2, the resource reserve is 970 Mt, and the main mining area is No. 2 coal seam.

The mining length of the 205 working face is 3000 m and working face length is 260 m. The overburden rock thickness is 180~380 m. The main coal seam is No. 2 coal, strip bright coal. The coal seam has simple occurrence conditions and no other geological structures. Only one layer of gangue is distributed in some areas. The thickness of the gangue is 0.1 m, and the lithology of the gangue is mudstone. The thickness of the coal seam is 2.5–5.7 m. The direct bottom plate is dark gray mudstone, which is lumpy and 1.3–1.5 m. The formation tendency is 1-2°.

The 205 working face is simple in structure. Within the scope of the working face, the rock layer is nearly horizontal and undulating no more than 4°. The general trend is lower in the middle and higher on both sides. The hydrogeological conditions of the 205 working face are simple, and locally, there will be coal seam fracture water.

2.2. Selection Principle. Through the actual monitoring of the 205 working face, it is found that 78% of the gas in goaf is from surrounding rock gas, so the method of drilling and mining is adopted to solve the gas problem. By measuring the development range of the gas migration channel, the proportion of high hole extraction, roof extraction, and floor extraction was determined to be 31%, 41%, and 28%, respectively. In order to achieve multidimensional full coverage in space, it is proposed to carry out three-dimensional comprehensive gas extraction in space by implementing directional long drilling holes in the roof and floor and, at the same time, to achieve "premining (extraction), in-mining, and postmining" gas exploration and extraction mode in terms of time. In order to fundamentally solve the problem of mine gas, it is necessary to improve the efficiency of mine gas extraction and provide strong support for the realization of the intrinsic safety of gas control in mine mining, as shown in Figure 1.

3. Key Parameters of Directional Drilling of the Surrounding Rock

3.1. The Influence Area of Roof Hole Mining

3.1.1. Analysis of Roof Deformation and Failure. Before being affected by mining, the original stress of the formation is in a dynamic equilibrium state. Goaf is formed after coal mining, which destroys the original stress balance conditions of the surrounding rock and causes the stress redistribution of the surrounding rock until it reaches a new mechanical balance state. And, in the coal, itself, the surrounding rock produced the relief pressure (pressure reduction) and stress concentration phenomenon. These changes in stress result in changes in the fracture rate of floor rock strata. The area where the stress is less than the original stress is the pressure relief area. At the same time, after coal mining, the rock layer around the production space loses support and gradually moves, bends, and breaks into the goaf. This process gradually expands outward, upward (roof), and downward (floor) from the stope with the continuous advancement of the mining face. Due to the different position of the roof and floor, the deformation and failure under force are different.

The movement and failure of the surrounding rock is a complicated process in time and space. Through long-term observation, it has been proved that the movement and destruction of the overlying strata (roof) have obvious zonation, and its characteristics are related to geology, mining, and other factors. Under the condition of mining the gently inclined medium-thick coal seam with the full strike-wall caving method, as long as the buried depth reaches a certain depth (the ratio of mining depth to mining height is greater than 40), there will be three representative parts of roof overburden failure and movement, which are, respectively, referred to as the caving zone [13], fracture zone [14], and curved subsidence zone [15, 16], from the bottom to the top.

According to practical experience, the overburden rock in the caving zone is seriously damaged, and drilling is prone to borehole accidents. The separation fractures are the main part of the bent subsidence zone, which is not suitable for the extraction between gas layers. The influence of rock fracture in the fracture zone on the construction borehole is less than that in the caving zone, and the fracture is more developed than that in the curved subsidence zone. Therefore, the favorable stratum for the drainage arrangement of the high-gas borehole is selected in the fracture zone. According to

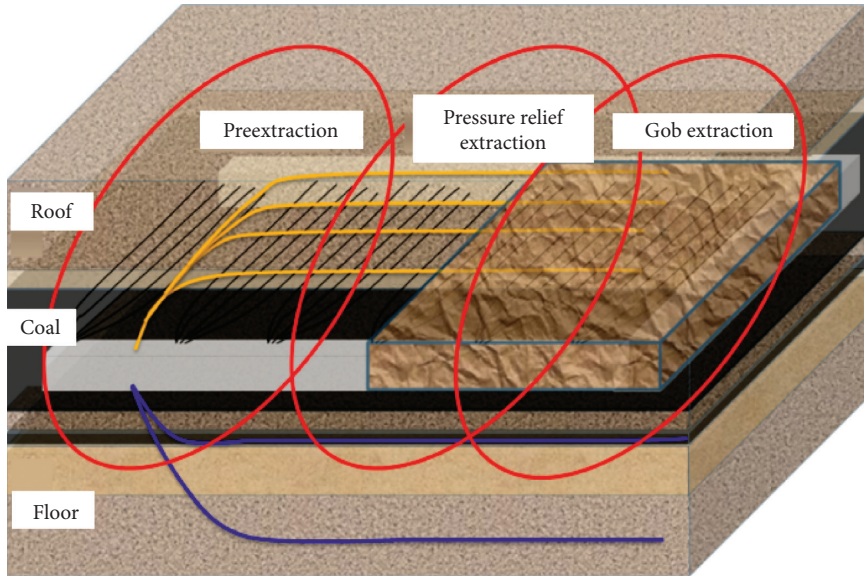

Figure 1: Coal, oil, and gas symbiotic mine three-dimensional comprehensive extraction mode.

the observation and test results of the crack zone in Sipan District of Huangling No. 2 coal mine in 2012, the height range of the crack zone in the fully mechanized coal face is 20~66 m under the condition of a certain mining height and little lithology change of the roof.

3.1.2. Analysis of Floor Deformation and Failure. After coal mining, under the dynamic comprehensive action of mining stress, the floor of the coal seam appears to have deformation and failure in different degrees. The changes in stress will lead to changes in the fracture rate of floor rock strata, which will lead to the formation of vertical tensile fractures, stratified fractures, shear fractures, and so on. Because the bottom plate is in the lower layer, the failure deformation of the bottom plate during mining is weaker under the influence of gravity than that of the top plate, so the change of its stress state is analyzed first.

(1) Model Establishment. FLAC (Fast Lagrangian of Continua), a large-scale geotechnical engineering special software designed and developed by the American ITASCA Consulting Group, can be used to solve the stress analysis of deep foundation pits, slopes, foundations, dams, tunnels, underground stopes, and caverns. It can also be used for dynamic analysis. The "explicit Lagrangian" algorithm and "hybrid-discrete partitioning" technology adopted by FLAC3D can simulate the plastic failure and flow of materials very accurately. Since there is no need to form a stiffness matrix, it can solve large problems based on a small memory space. The mining of coal seam belongs to the damage range of the three-dimensional geological space size. Due to the use of automatic inertia and automatic damping coefficient, it overcomes the limitation of small-time steps and damping problems in explicit formulas. Therefore, FLAC3D is one of the most ideal tools for solving 3D geotechnical problems. And, FLAC3D software was used for analysis of floor deformation and failure in this work.

Taking the floor of No. 2 coal seam of the 205 working face as the research object, the working face tends to be 280 m long, and the trend of simulated mining is 120 m. Coal mining is carried out along the model strike. The strike length of the model is 400 m, the trend width is 579 m, the vertical direction is 191 m, and the thickness of No. 2 coal seam is 3.2 m. The average buried depth of No. 2 coal seam is 610 m within the calculation range, and the rock layer of No. 2 coal seam is 105 m above it. The rock mass from the top to the surface of the model applies self-weight to apply vertical load, and the coal seam floor includes a rock layer model of 86 m thick. The thickness of the loose layer and overburden layer is replaced by compensation load. The original stress field is the gravity field. The Mohr–Coulomb criterion is chosen as the rock failure criterion. To eliminate the boundary effect, a 140 m width boundary is left at both ends and a 150 m boundary is left at both ends of the trend of the model. All constraints are applied to the lower end of the model. The left and right sides constrain the displacement in the X direction, respectively, while the front and rear sides constrain the displacement in the Y direction. The upper end face is the free end. The top surface of the model was subjected to overburden stress, and the vertical stress outside the initial overburden model was calculated as 12.4 MPa according to the calculation formula of rock body weight ($P = \gamma H$).

The mechanical parameters of the top and bottom slabs of the 2# coal seam in the experimental mine were obtained from laboratory tests, and the model parameters in the numerical simulation were determined according to the mechanical properties of the coal rocks. Obtain the physical parameters of simulated strata, as shown in Table 1.

(2) Simulation Calculation. The simulated mining length is 120 m, and the mining is carried out step by step. Each step

Table 1: Simulated formation physical parameters.

Lithology	Bulk modulus (GPa)	Shear modulus (GPa)	Cohesion (MPa)	Internal friction angle (°)	Tensile strength (MPa)	Density (Kg/m^3)
Mudstone	1.51	0.65	2	20.9	1.26	2400
Silt	4.46	1.12	4	24.9	2.13	2500
Fine sand	5.28	1.65	6	25.6	2.5	2600
Coal seam	0.57	0.24	1.2	18	1.2	1400

has a recovery of 20 m and a recovery width of 280 m. The accumulative amount of excavation is 6 steps, and 120 m of excavation is completed. Bottom plate depth of the middle monitoring model is as follows: 1 m, 5 m, 15 m, and 40 m. By simulating the process of coal mining, the stress distribution of the floor, the change of floor displacement, and the change of the failure zone are monitored during the mining process.

(3) Analysis of Simulation Results. When the stopping surface is pushed forward for 20 m, pressure relief appears on the roof and floor on the working strike section, with a vertical depth of about 8 m, as shown in Figure 2. When the pressure relief range and depth of the stoping surface are gradually expanded to 80 m, the vertical pressure relief depth is about 48 m. When it reaches 120 m, the pressure relief range and degree of the top and bottom are basically stable, and the vertical depth is about 60 m. It can be seen from the simulation results that, under the influence of mining, the stress of the coal seam and its floor is under the state of pressure (rising), and the floor coal and rock mass are compressed in the pillar area. In the goaf, the stress of floor rock strata is in the state of pressure relief (decrease), and the floor coal and rock mass expand. Moreover, with the continuous mining activities, the pressure relief range of floor rock strata keeps increasing. When the pressure relief range increases to a certain extent, the pressure relief range is basically stable. In addition, with the collapse and compaction of roof overburden, the gravity load of floor overburden tends to be stable, and the stress recovery zone appears corresponding to floor abutment pressure. However, the coal that is not affected by the mining action has no change in stress. Therefore, in the normal mining stage, the coal and rock on the working face floor appears in the original stress area, stress concentration area (compression area), pressure relief area (expansion area), and stress recovery area (compaction area).

This is a description of the failure process of the formation, divided into four stages: advanced stress concentration—concentrated compression—stress release—stress recovery and recompression [17–19]. The overlying rock collapse is accompanied by rock fragmentation, and during the destruction of the rock, the surrounding stress is constantly changing, so back to the formation of delaminated fissures and broken fissures. Here, we mainly analyze the failure process of stress release of floor rock strata. According to the data analysis of different vertical depth detection points of the model (Figure 3), the same depth line has obvious zoning on the trend.

The middle area is relieved of pressure. According to the different depth detection point data analysis of the model (Figure 4), the same depth line has obvious partition, intermediate regional pressure, and two-side coal region stress concentration, and the remote area of both sides is restored to the original stress, overall with " ear U" type. With the advance of the working face, the pressure is gradually relieved, and the shallow depth line starts to change in a large and drastic range and then gradually decreases and tends to be stable (Figures 4(a)–4(c)). On the direction of the deep depth line, the change amplitude is small at the beginning, then large, and then small. After a certain distance of the working face, compaction and stress recovery begin to occur (Figure 4(d)). It indicates that the shallow part is the first to be damaged, while the deep part is the first to be deformed after the shallow part is damaged. After the failure, the stress changes gradually, and after the working face advances a certain distance, compaction begins to occur along with the collapse of the roof. By comparing the stress variation patterns of different depth lines, it is obvious that the shallow shape curve is sharp, and the deep one is smooth, indicating that the shallow stress variation of the coal floor is drastic. In the deep part, the change is gentle, indicating that the shallow part is violent in failure and deformation, while the deep part is relatively slow.

By analyzing the plastic failure areas of models with different advancing distances on the stoping face, the failure areas of floor rock strata can be intuitively obtained, as shown in Figure 4. With the continuous advance of the stope working face, the floor failure area in the inclined section of the working face is basically distributed in the shape of M, with the two channels with the greatest damage degree of the floor, followed by the middle area. After the stoping surface exceeds 80 m, the failure depth of the floor increases slowly, and the pressure relief range reaches a stable base when the stoping reaches 100 m. The maximum failure depth of the floor is about 40 m.

3.2. Gas Analysis of the Surrounding Rock

3.2.1. Roof Gas Sandstone Layer. The sandstone thickness of Qili Town is between 3 and 27 m, and the whole working face is distributed. The 4–6 section is relatively thick, reaching 25 m or more, and both sides gradually become thinner, from the 8 section to the open-eye section of about 5 m. In Qili Town, the distance between the sandstone and the coal roof is zero from the 5th lane to the 7th lane, which is in direct contact with the coal seam. The distance between the sandstone and the No. 2 coal roof is less than 18 m. The elevation of the top surface is 740~800 m, and the elevation difference is about 60 m. From the entrance to the lane, it

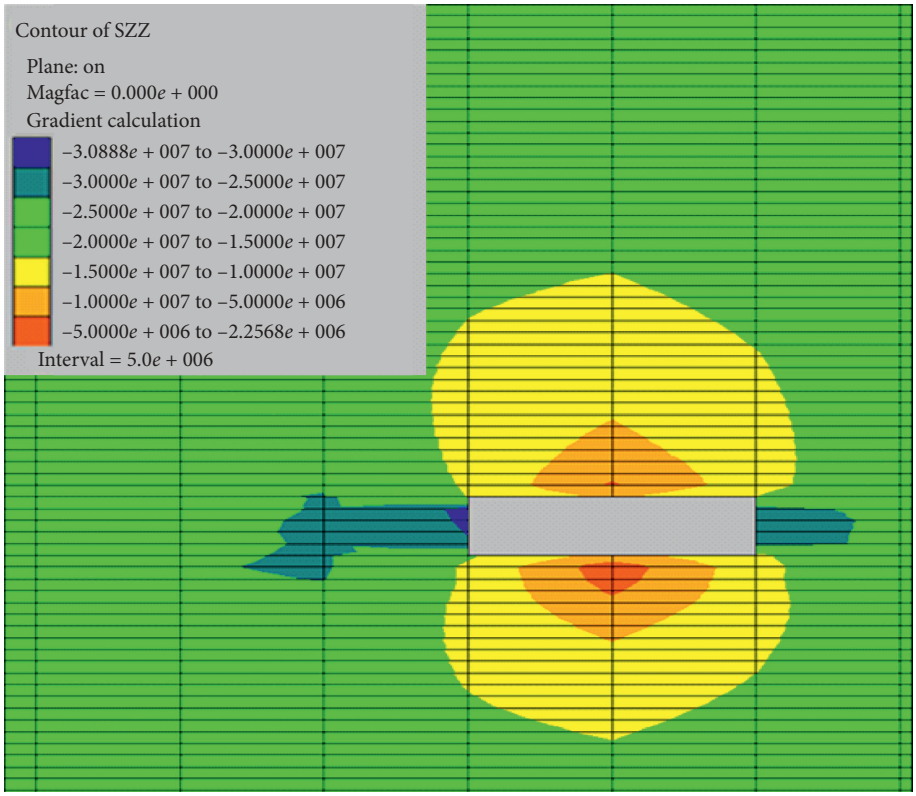

(a)

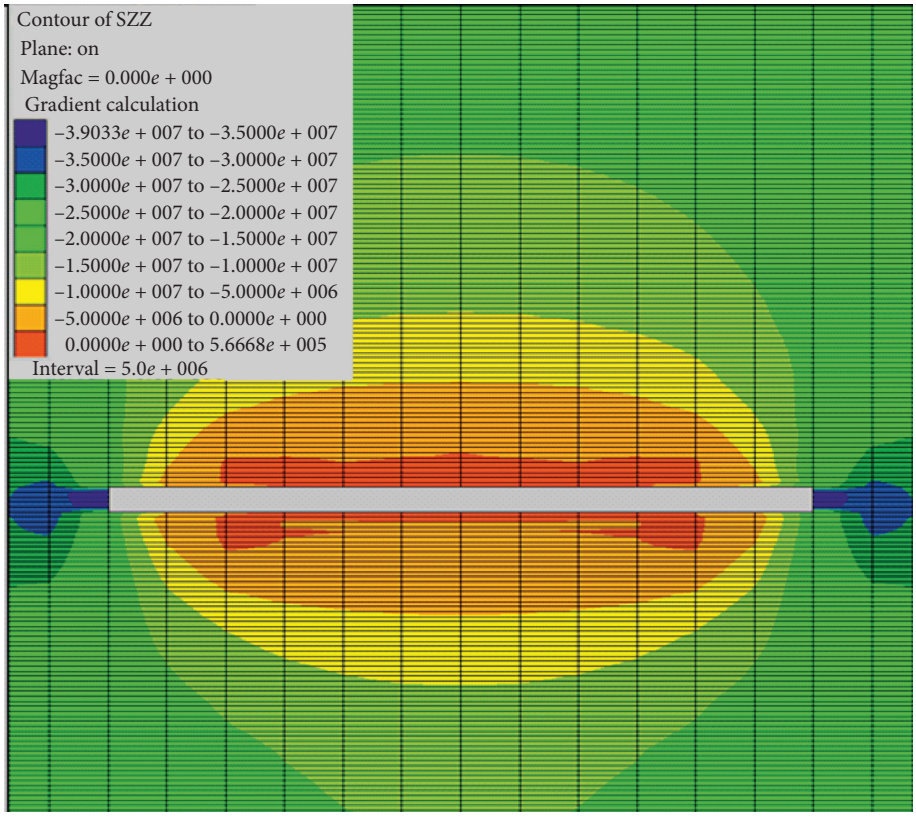

(b)

Figure 2: Continued.

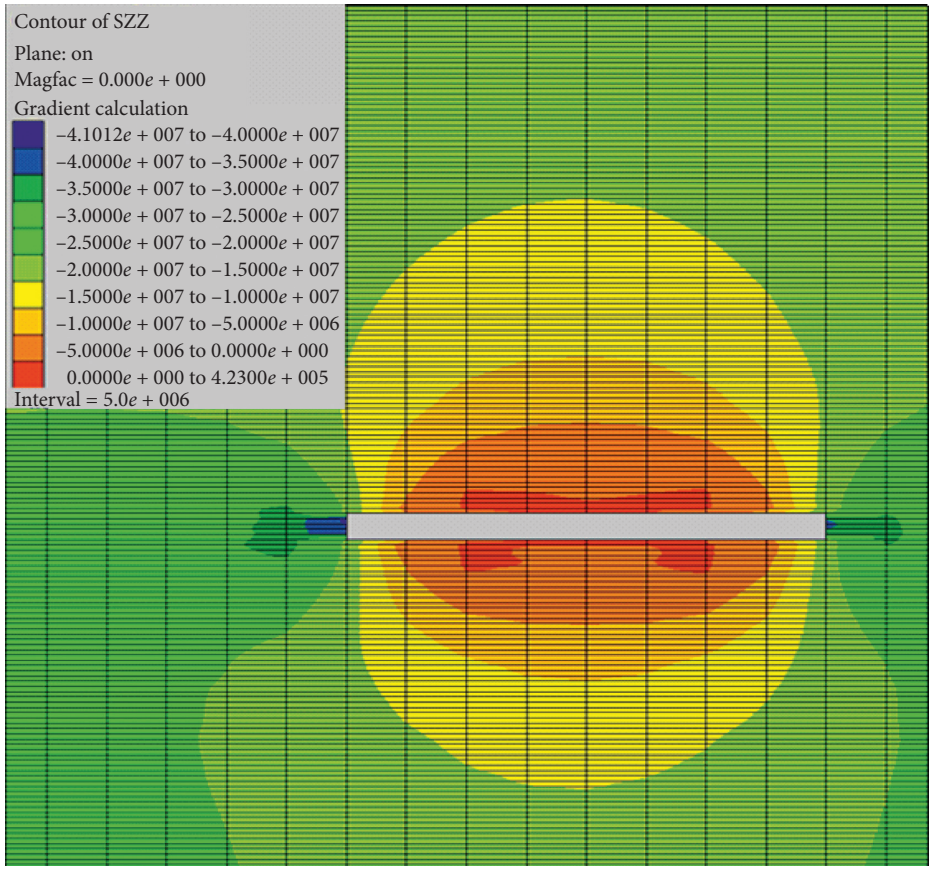

(c)

Figure 2: Vertical stress distribution of the floor at different mining distances on the working face. (a) 20 m. (b) 80 m. (c) 120 m.

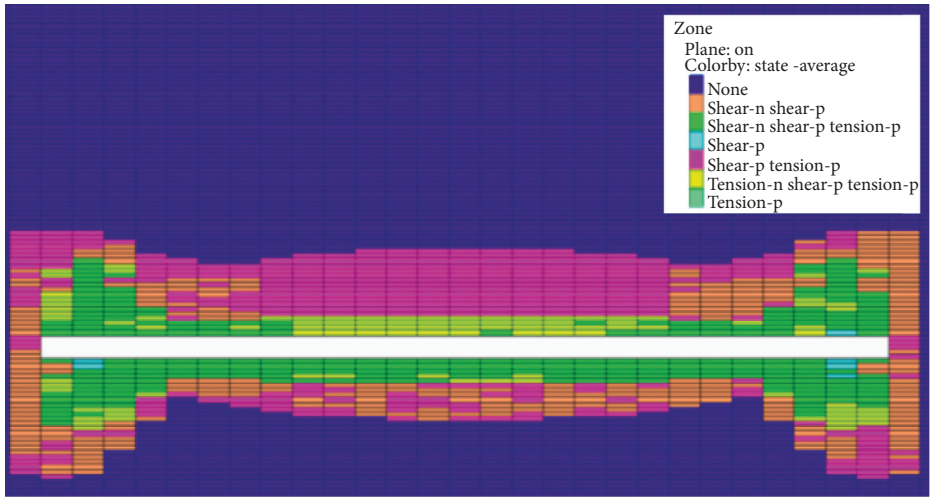

(a)

Figure 3: Continued.

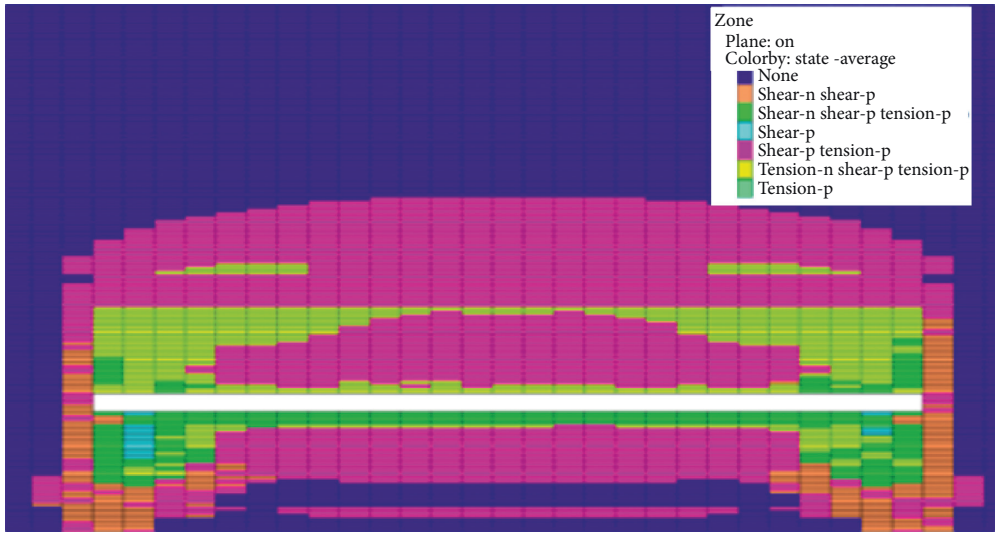

(b)

Figure 3: Working face at different mining distances tends to floor failure area distribution. (a) Mining 80 m. (b) Mining 120 m.

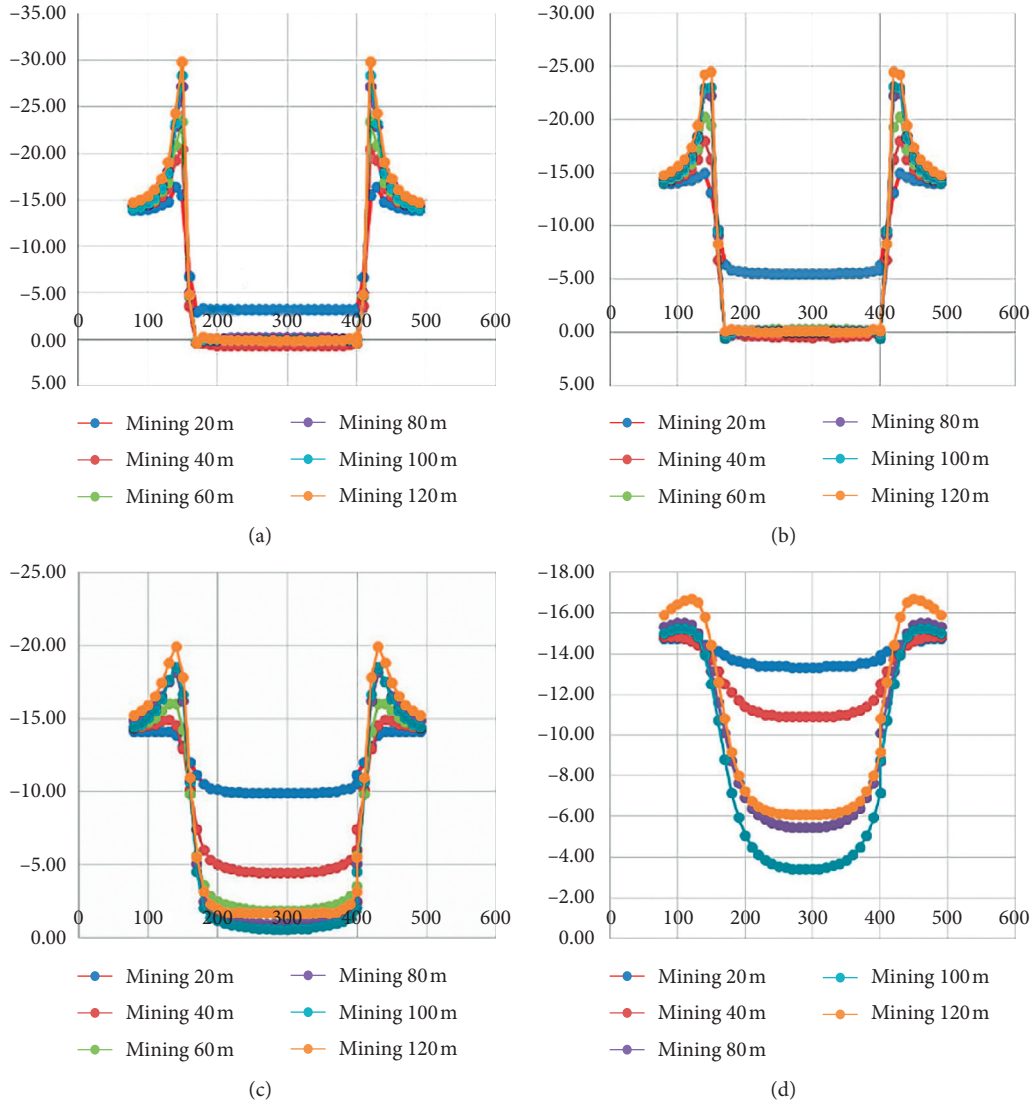

Figure 4: Stress variation under the same floor depth with different stoping distances. (a) Floor 1 m. (b) Floor 5 m. (c) Floor 15 m. (d) Floor 40 m.

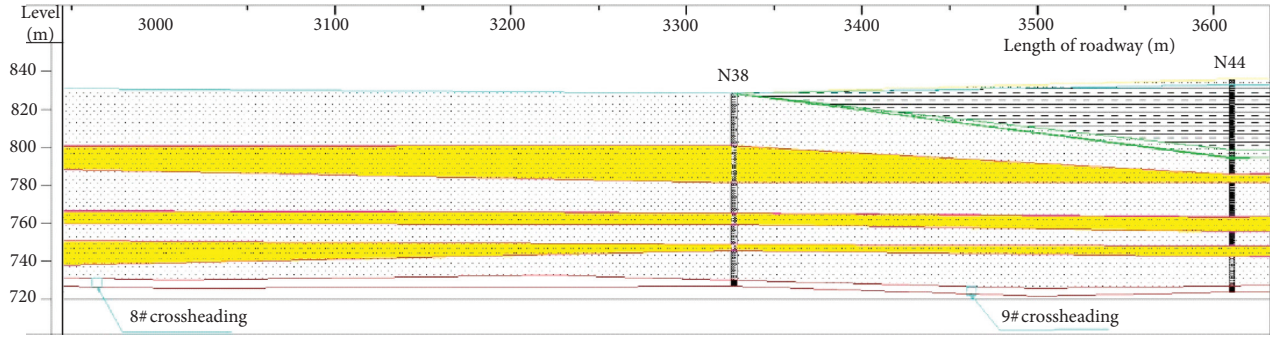

Figure 5: Regional section of roof formation.

presents a downward trend. Qili Town sandstone, whose porosity is less than 5% and permeability is 0.59×10^{-4} m^2 on average, belongs to the tight reservoir.

Select the surface exploration borehole near the 205 working face to make the seam roof connecting well with the section, as shown in Figure 5. It can be seen that, in addition to the Qili Town sandstone, there are two layers of fine-grained sandstone on the top of the coal seam. The first layer is the two-stage two-cycle fine-grained sandstone layer with a thickness of about 6.4 m and a distance of about 30 m from the coal seam. The other layer is a three-cycle fine sandstone layer of the second extension, with a thickness of 6~14 m and a relatively large spacing of 55~68 m from the coal seam.

3.2.2. Floor Gas-Bearing Sandstone Layer. There are four layers of gas-bearing sandstone within 50 meters of the vertical depth of the floor of the 205 working face. The first layer between No. 2 coal and No. 3 coal appears within 2600 m of the roadway, where the spacing between No. 2 coal and No. 3 coal becomes larger. The thickness is 0~7.9 m, which is close to the spacing between No. 2 coal seams, and most areas are less than 1 m.

The second floor of Fuxian Formation has one floor at 1600 m with a thickness of 0~11.1 m and a spacing of 0.7~16.5 m between it and No. 2 coal seam. Another layer appears at the bottom of 2200 m, with a thickness of 0~7.6 m, and the distance between it and No. 2 coal seam is about 25 m. The lower sandstone of Fuxian Formation belongs to a tight reservoir with porosity less than 5% and average permeability of 0.48×10^{-4} m^2.

The first floor of the Wayaobao Group began to appear from the detection hole at the entrance of the alley. By about 2000 m, the distance between it and No. 2 coal had become larger. It is predicted from the exploration in the whole region that the contour lines of the top elevation are distributed continuously in the 205 working face regions. The contour lines of the top surface show a trend of gradually decreasing from the alley entrance to the interior. The thickness is 10~23 m, and the distance between the top elevation and No. 2 coal seam is 25~35 m. The sandstone in Wayaobao Formation belongs to a tight reservoir with porosity less than 5% and permeability average 0.48×10^{-4} m^2.

3.3. The Optimal Scheme of the Long Hole in the Surrounding Rock. Based on the analysis of the influence of upper mining, it can be seen that, under the condition of certain mining height and little lithology change of the roof, the height range of the roof fracture zone in the fully mechanized coal mining face is 20~66 m. Taking the No. 2 coal seam floor of the 205 working face as the research object, the failure depth of the floor is analyzed through numerical simulation, and the range is 6~40 m.

The distance between Qili Town sandstone and No. 2 coal seam in the roof Yan'an formation 2nd section is 0~28.81 m, and the distance between No. 3 coal seam and No. 2 coal seam in the floor is 0~14.31 m. The average spacing between the gas-bearing sandstone beds between No. 2 coal seam and No. 3 coal seam, the two gas-bearing sandstone beds in Fuxian Formation, and the gas-bearing sandstone at the top of the Wayaobao Group and coal seam No. 2 is all less than 40 m. Therefore, these reservoirs can be used as the primary consideration for the layout of directional long drilling. Both the roof and the floor contain multiple gas reservoirs within the vertical depth affected by mining. The drilling should be preferentially arranged in the reservoir closer to No. 2 coal. In this way, it is convenient to intercept the gas which is transported from the relief pressure to the stoping space of the gas-bearing layer at the far end of extraction under the influence of working face mining. Through comprehensive analysis, the layout of the comprehensive three-dimensional extraction hole is determined as follows.

3.3.1. Roof Directional Long Hole. It is mainly aimed at the gas-bearing stratum of Qili Town sandstone, controlling the upper corner gas of goaf, and retaining the downward migration gas of the upper gas-bearing stratum under the influence of mining. In addition to minimizing air leakage on the working face, a circulation channel for gas in goaf should also be provided. Negative pressure extraction [20–25] is carried out in the construction drainage hole to drain the goaf gas under the effect of the pressure gradient, which provides a circulation channel for the gas in the goaf. When the pumping effect is good, the problem of upper corner gas can be solved well. According to the distribution of gas-bearing strata in Qili Town sandstone and the influence of mining, the boreholes are arranged

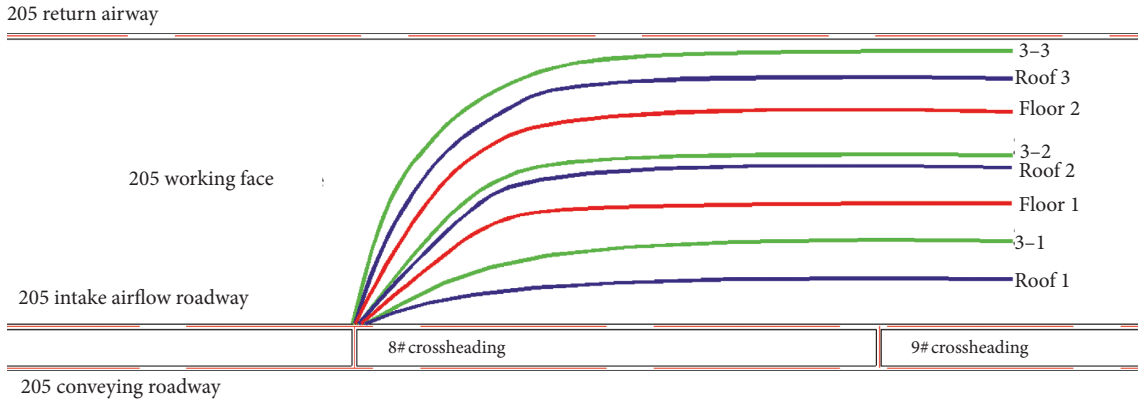

Figure 6: Layout of the directional long hole in the surrounding rock.

Table 2: Design parameters of three-dimensional pumping directional drilling.

Long borehole on top of roof					
No.	Starting position (°)	Primary dip (°)	Long hole (m)	Distance from return airway (m)	Distance from No. 2 coal top (m)
Roof 1	303.16	16	621	240	20
Roof 2	313.16	16	679	140	30
Roof 3	323.16	16	748	40	40

Table 3: Design parameters of three-dimensional pumping directional drilling.

Long hole along the No. 3 coal seam				
No.	Starting position (°)	Primary dip (°)	Long hole (m)	Distance from return airway (m)
3-1	295.16	−5	631	200
3-2	305.16	−5	688	110
3-3	315.16	−5	774	10

Table 4: Design parameters of three-dimensional pumping directional drilling.

Long bottom hole					
No.	Starting position (°)	Primary dip (°)	Long hole (m)	Distance from return airway (m)	Distance from No. 2 coal bottom (m)
Floor 1	298.16	−9	656	160	8
Floor 2	308.16	−9	722	70	8

within the vertical depth of 20~40 meters, and the sandstone is spread in Shunqili Town including the floor gas-bearing sandstone layer and No. 3 coal seam directional long hole [26–30].

3.3.2. Floor Directional Long Hole. The directional long drilling hole of the bottom plate selection is arranged in the sandstone gastrointestinal gas in the lower part of the rich county. The gas in the layer can be pumped, and the gas that moves upwards affected by the mining can also be pumped. Which cannot only extract the gas of this layer but also extract upward migration gas of the sandstone gas-bearing layer at the top of Wayaobao formation affected by mining. According to the distribution of sandstone at the lower part of the Fuxian formation in the region, the borehole track is designed to be arranged in the layer 8~15 m away from the bottom of the No. 2 coal mine, and the sandstone at the lower part of the Shunfu Formation is distributed. The directional long drilling hole of No. 3 coal seam is spread along the direction of the working face, and the gas is mainly extracted from No. 3 coal seam.

4. Analysis of the Implementation Effect of Directional Drilling

4.1. The Layout of the Borehole. The selection of directional long borehole parameters mainly considers the layout of the roadway, the drainage period of the directional long borehole, the coverage area of the borehole, and the cost of construction. Combining with the distribution of the cracks in the mined-out area and the distribution of oil-type gas

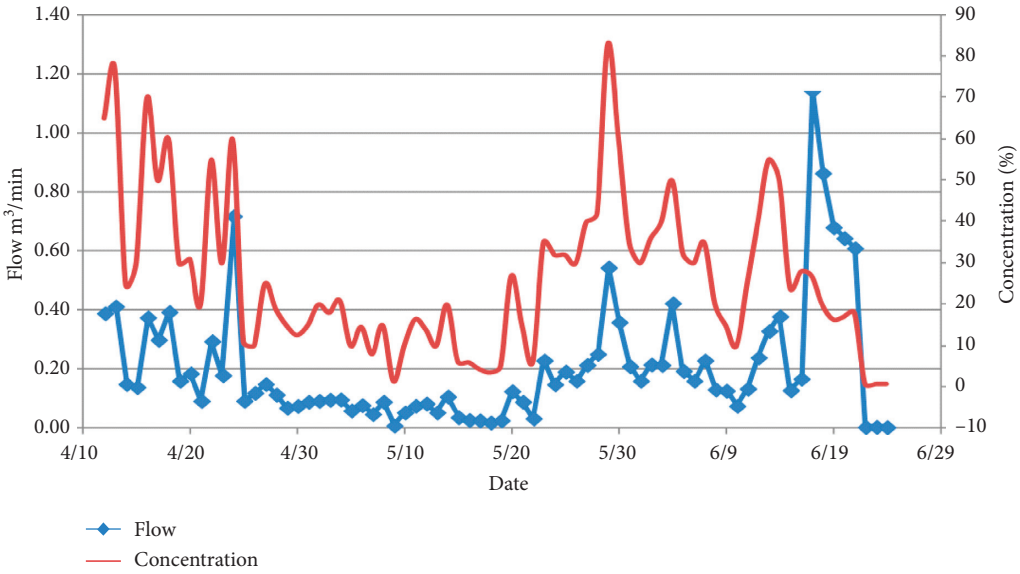

Figure 7: Extraction concentration and pure flow curve of the roof borehole 1-1.

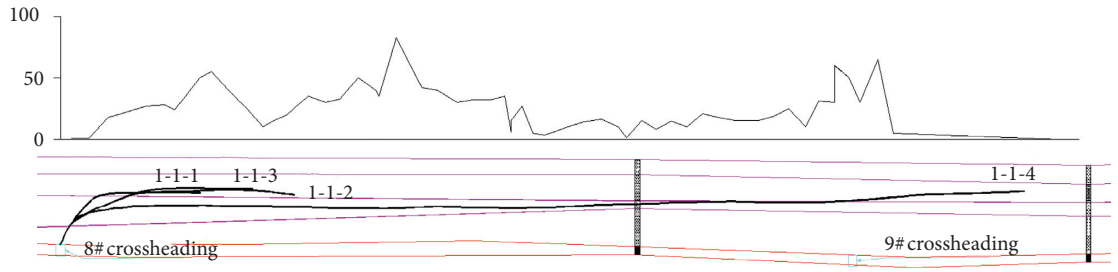

Figure 8: Corresponding figure of extraction concentration of the roof borehole 1-1 and borehole track.

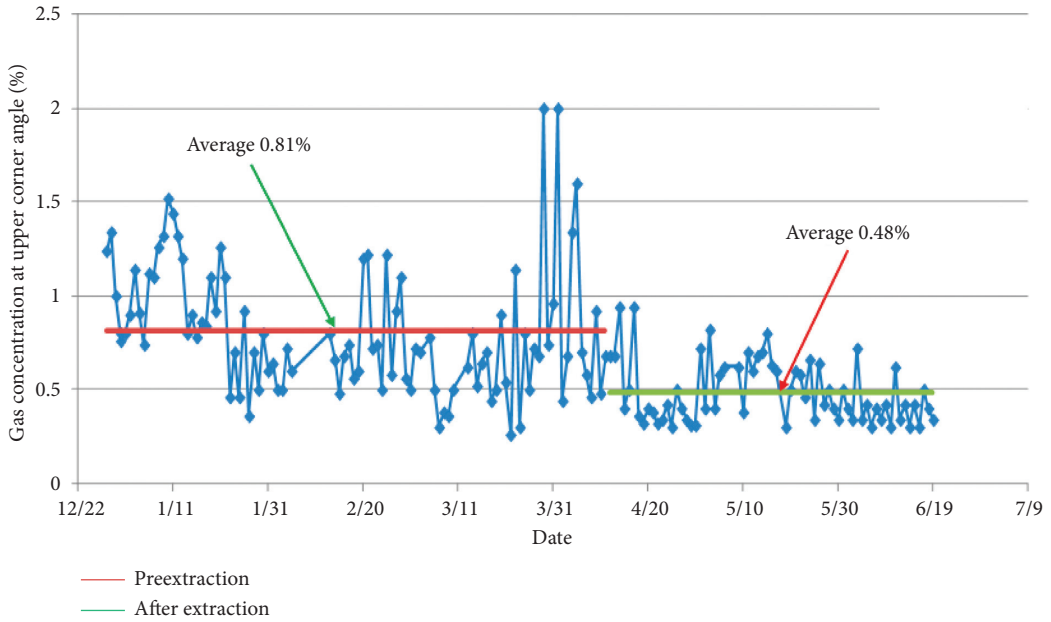

Figure 9: Upper-corner gas concentration tracking curve.

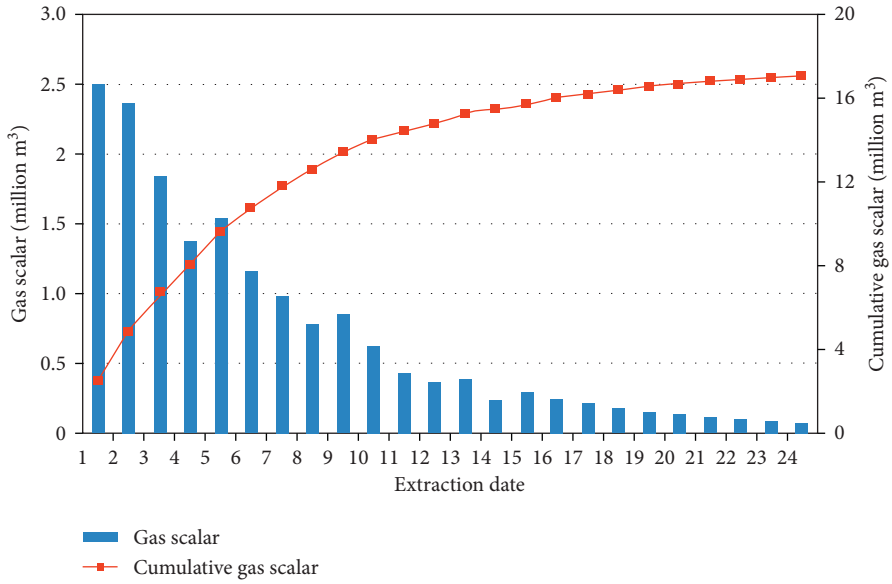

Figure 10: Gas extraction purity and cumulative extraction purity of borehole No. 1-1.

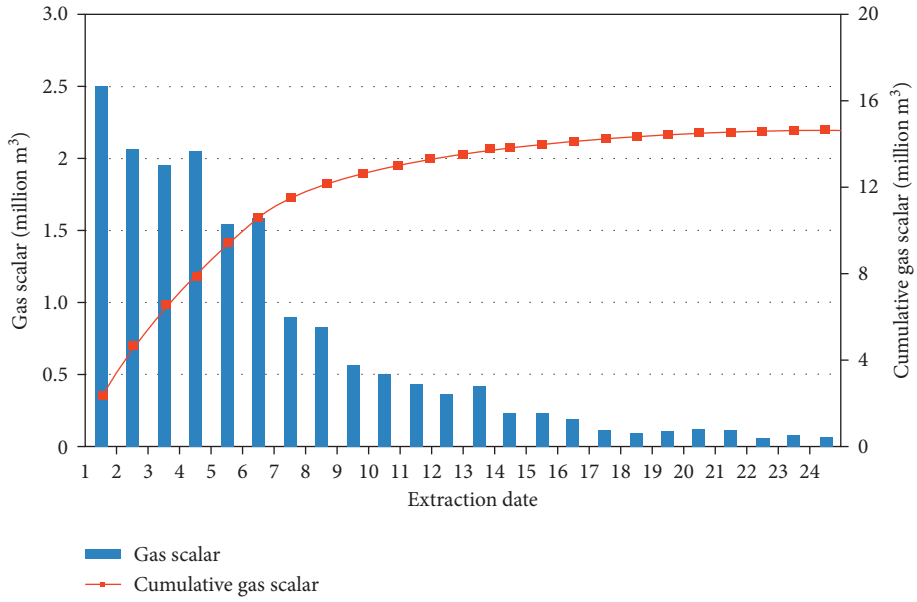

Figure 11: Gas extraction purity and cumulative extraction purity of boreholes No. 1-2.

reservoirs, the plan layout of the directional long boreholes, the construction trajectory, the construction location, and the spacing are studied. According to on-site construction conditions, it is designed to arrange the roof, floor, and directional drilling of the 3 coal along the layer in the 205 working face with 8 lanes to carry out premining predrainage and in-mining mining drainage and postmining goaf drainage. Drilling to the bearing arrangement is shown in Figure 6. Design parameters are shown in Tables 2–4. In order to understand Figure 6, refer to the data in Tables 2–4.

4.2. Inspection of the Extraction Effect

4.2.1. Directional Drilling of Roof, Floor, and No. 3 Coal Seams. According to the roof borehole 1-1, methane extraction concentration averaged 28%, methane extraction purity averaged 300 m^3/d, and gas extraction from surrounding rocks accumulated to nearly 22,000 m^3, as shown in Figure 7. Corresponding to the drilling concentration and the working surface and the drilling distance, as shown in Figure 8. The placement of directional long boreholes at

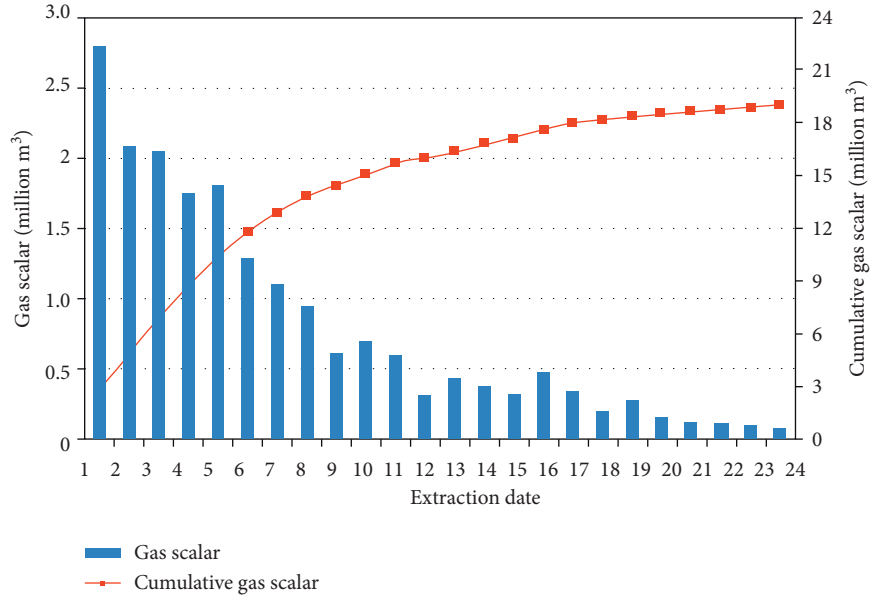

Figure 12: Gas extraction purity and cumulative extraction purity of borehole No. 1-3.

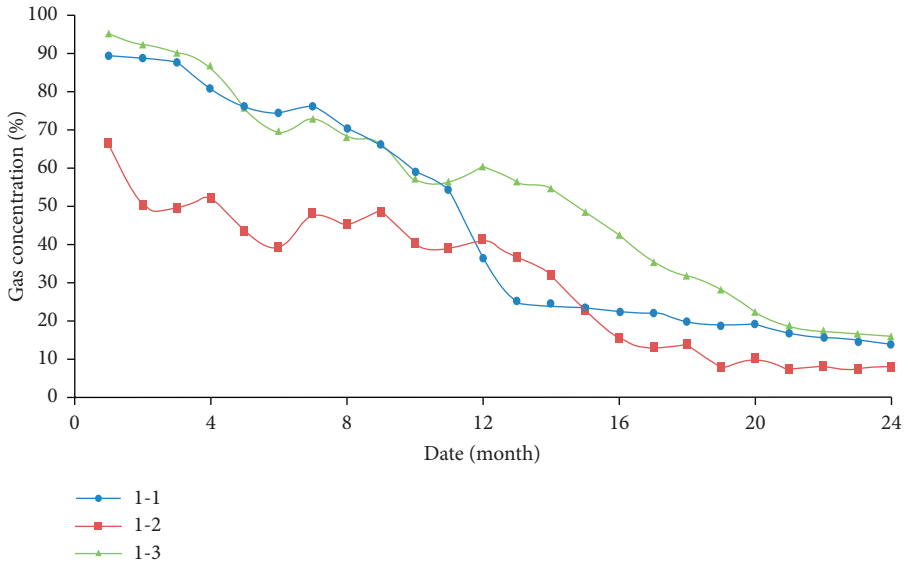

Figure 13: Concentration of borehole gas in No. 1 drilling field.

different locations backfires because of the different stress changes in the final hole location, thus affecting the efficiency of gas extraction. The drainage concentration of the borehole track is not high in the upper siltstone layer and significantly increases when it enters the Qili Town sandstone member.

By tracking the concentration of corner gas on the working surface, a comparison was made between the long drill before and after extraction. As shown in Figure 9, the average statistical concentration was 0.81% in the first 3 months before it entered the roof drilling area and 0.48% in the second month after the extraction of the long drilling hole, which decreased by 41%, indicating a significant decrease.

4.2.2. Directional Drilling of This Seam. Within the range of 0~400 m from the stop-mining line to the auxiliary lane 205, a total of 3 regional prepumping chambers shall be constructed as the regional prepumping drilling field, and 3 long boreholes shall be arranged in each regional prepumping chamber. From Figures 10–13 , it can be seen that the gas concentration of No. 1-1 borehole drops to 14.0%~89.0% after 24 months, the gas purity is 0.071~25,008 m^3/month, and the cumulative gas extraction is 170,200 m^3.

The gas concentration of No. 1 and No. 2 boreholes was reduced to 7.0%~66.0%, the gas extraction purity was 0.057~20,008 m^3/month, and the cumulative gas extraction volume was 136,500 m^3. The gas concentration of No. 1–3 drilling holes was reduced to 16.0%~95.0%, the gas

extraction purity was 0.079~27,910 m^3/month, and the cumulative gas extraction was 189,700 m^3, as shown in Figure 10.

Figure 11 shows that the gas concentration of No. 2-1 drilling holes was reduced to 16.8%~90.0%, 16.8%~90.0%, the gas extraction purity was 0.011~28,680 m^3/month, and the total extraction volume was 194,900 m^3. The gas concentration of No. 2-2 borehole was reduced to 16.5%~87.0%, the gas extraction purity was 0.082~28,920,000 m^3/month, and the total extraction volume was 196,500 m^3. The gas concentration of No. 2-3 boreholes was reduced to 14.4%~ 48.0%, the gas extraction purity was 0.051~ 8,04 m^3/month, and the total extraction volume was 122,600 m^3.

The gas concentration of No. 3–1 drilling hole was reduced to 13.4%~92.4%, the pure gas extraction was 0.079~27,994 m^3/month, and the total gas extraction was 188,500 m^3, as shown in Figure 12. The gas concentration of No. 3-2 borehole was reduced to 15.2%~80.0%, the gas extraction purity was 0.067~23.5 million m^3/month, and the total extraction volume was 159,700 m^3. The gas concentration of No. 3-3 borehole was reduced to 17.0%~85.0%, the gas extraction purity was 0.068~23,87 m^3/month, and the total extraction volume was 162,200 m^3. The total gas extraction volume of the 9 prepumping boreholes is 1.520,800 $m^{3,}$ which shows a good extraction effect.

The original gas content in the area 0~400 m from the auxiliary lane 205 to the stop-production line is 3.01 m^3/t. Then, after 2 years of prepumping, the gas content of the coal seam after regional prepumping is 1.56~1.73 m^3/t, and the prepumping rate is 42.52%~48.17%. The gas pressure was reduced from 0.65 MPa to 0.19~0.28 MPa, as shown in Figure 13.

5. Conclusions

(1) Based on the study of the oil-type gas reservoir and the influence range of mining on the working face in the surrounding rock, the paper puts forward the optimization method of the directional long borehole layout of the surrounding rock and the method of borehole layout with comprehensive consideration of the influence of mining on the failure of the roof and floor and the distribution of surrounding rock gas-bearing reservoirs. The roof borehole is arranged in the vertical depth of 20~40 meters, and the relevant parameters and directional borehole trajectory are determined.

(2) By tracking and monitoring the data of 1164 groups of three-dimensional extraction boreholes in each drilling field, the pure methane extraction from roof boreholes averaged 98~300 m^3/d, and the methane extraction concentration averaged 17%~35%. The average pure methane extraction from the floor borehole is 76~178 m^3/d, and the average methane extraction concentration is 3.1~26%. Methane extraction from No. 3 borehole averaged 56~190 m^3/d, and methane extraction concentration averaged 10%~66%.

(3) The correlation between the extraction data and the exposed layer and the layout of the borehole was studied, and the gas concentration in the corner of the working surface before and after extraction was compared. It can be seen from the concentration and quantity of borehole extraction that the integrated three-dimensional extraction has obvious effects in revealing extraction before relieving pressure during and after extraction. The concentration of gas in the upper corner drops from 0.81% to 0.48%, with a decrease of 41%. It is proved that directional drilling-integrated gas preextraction is a technical method worthy of popularization.

Data Availability

The data are available and explained in this article; readers can access the data supporting the conclusions of this study.

Conflicts of Interest

The authors declare no conflicts of interest.

Authors' Contributions

The manuscript was approved by all authors for publication.

Acknowledgments

This research was funded by the Natural Science Basic Research Program of Shaanxi Province (no. 2019JLZ-08).

References

[1] H. F. Wang, Y. P. Cheng, W. Wang, and R. Xu, "Research on comprehensive CBM extraction technology and its applications in China's coal mines," *Journal of Natural Gas Science and Engineering*, vol. 20, pp. 856–863, 2014.

[2] X. P. Jiang, S. W. Fan, Z. H. Cheng et al., "A three-zone integrated gas Control Model based on joint pumping from top to bottom," *International Journal of Coal Science & Technology*, vol. 46, pp. 107–113, 2016.

[3] Y. P. Cheng and Q. X. Yu, "Development of regional gas control technology for Chinese coalmines," *International Journal of Mining and Mineral Engineering*, vol. 5, no. 1, pp. 383–390, 2007.

[4] Y. P. Cheng, J. H. Fu, and Q. X. Yu, "Development of gas extraction technology in coal mines in China," *International Journal of Mining Science and TechnologyInternational Journal of Mining Science and Technology*, vol. 26, pp. 127–139, 2009.

[5] X. H. Bai, C. F. Wu, X. L. Liu, and Y. B. Li, "Analysis of the tempo-spatial effects of hydraulic fracturing by drilling through underground coal mine strata on desorption characteristics," *Energy Science & Engineering*, vol. 7, pp. 476–491, 2019.

[6] F. T. Wang, T. Ren, S. H. Tu, F. Hungerford, and N. Aziz, "Implementation of underground longhole directional drilling technology for greenhouse gas mitigation in Chinese coal mines," *International Journal of Greenhouse Gas Control*, vol. 11, pp. 38–43, 2012.

[7] J. Liu, T. Yang, L. Wang, and X. J. Chen, "Research progress in coal and gas co-mining modes in China," *Energy Science & Engineering*, vol. 8, pp. 7072–7089, 2020.

[8] H. Chae, K. Nagano, Y. Sakata, T. Katsura, A. A. Serageldin, and T. Kondo, "Analysis of relaxation time of temperature in thermal response test for design of borehole size," *Energies*, vol. 13, pp. 74–87, 2020.

[9] R. Zhou and B. Z. Yan, "Study on gas pressure calculation method of gas Flow rate in radial flow field of perforation hole," *Journal of Rock Mechanics and Geotechnical Engineering*, vol. 35, pp. 3147–3152, 2016.

[10] S. Yang, G. C. Wen, F. Z. Yan, M. J. Zhang, and X. S. Zhao, "Evaluating the maximum rate of penetration for drilling borehole in soft coal seam," *Energy Science Engineering*, vol. 8, pp. 345–354, 2020.

[11] M. F. Shakib, E. Detournay, and N. Wouw, "Nonlinear dynamic modeling and analysis of borehole propagation for directional drilling," *International Journal of Non-Linear Mechanics*, vol. 113, pp. 1442–1454, 2019.

[12] T. M. Jiang and H. D. Miao, "Prospect of the application of kilometer drilling rig in Jinmei Group," *Coal Mining*, vol. 15, pp. 17–20, 2003.

[13] L. Yu, D. L. Zhang, Q. Fang, L. Q. Cao, Y. Zhang, and T. Xu, "Face stability of shallow tunnelling in sandy soil considering unsupported length," *Journal of Technology*, vol. 102, pp. 179–190, 2020.

[14] J. X. Hao, "Reasonable location determination of strike-high drainage roadway based on the development height of overlying rock fracture zone," *Journal of Safety Science and Technology*, vol. 16, pp. 75–81, 2020.

[15] X. G. Xia and Q. X. Huang, "Prediction model of rock strata movement in curved subsidence zone based on "four zones" division," *Rock And Soil Mechanics*, vol. 36, pp. 2255–2260, 2015.

[16] Z. Q. Xiong, G. M. Tao, and L. L. Zhao, "Regulation and control technology of roadway floor heave in curved subsidence zone of stope," *Coal Science and Technology*, vol. 41, pp. 43–46, 2013.

[17] K. G. Zheng and S. Q. Sun, "Simulation study on floor disturbance effect of coal and oil coexistence roadway tunneling," *Coal Science and Technology*, vol. 45, pp. 113–118, 2017.

[18] Z. J. Wang, "Optimization of surface drilling gas extraction Technology based on "O" ring theory," *Coal Mining*, vol. 22, pp. 96–101, 2017.

[19] D. F. Yang, Z. H. Chen, B. Li, X. Liu, and Q. Gao, "Numerical analysis of the characteristics of water migration in coal mine floor mining," *Coal Mining*, vol. 20, pp. 101–104, 2015.

[20] G. H. Ni, W. M. Cheng, B. Q. Lin, and C. Zhai, "Experimental study on removing water blocking effect (WBE) from two aspects of the pore negative pressure and surfactants," *Journal of Natural Gas Science Engineering*, vol. 31, pp. 330–346, 2016.

[21] Y. Wang, B. Zhang, S. H. Gao, and C. H. Li, "Investigation on the effect of freeze-thaw on fracture mode classification in marble subjected to multi-level cyclic loads," *Theoretical and Applied Fracture Mechanics*, vol. 111, Article ID 102847, 2021.

[22] Q.-X. Meng, W.-Y. Xu, H.-L. Wang, X.-Y. Zhuang, W.-C. Xie, and T. Rabczuk, "DigiSim-an open source software package for heterogeneous material modeling based on digital image processing," *Advances in Engineering Software*, vol. 148, Article ID 102836, 2020.

[23] Z. Tao, C. Zhu, M. He, and M. Karakus, "A physical modeling-based study on the control mechanisms of Negative Poisson's ratio anchor cable on the stratified toppling deformation of anti-inclined slopes," *International Journal of Rock Mechanics and Mining Sciences*, vol. 138, Article ID 104632, 2021.

[24] R. Jiang, F. Dai, Y. Liu, and A. Li, "Fast marching method for microseismic source location in cavern-containing rockmass: performance analysis and engineering application," *Engineering*, 2021.

[25] B. Li, R. Bao, Y. Wang, R. Liu, and C. Zhao, "Permeability evolution of two-dimensional fracture networks during shear under constant normal stiffness boundary conditions," *Rock Mechanics and Rock Engineering*, vol. 54, no. 3, pp. 1–20, 2021.

[26] Q. T. Zhang, S. Shi, and Y. F. Guo, "Application of integrated hydraulic fracturing anti-reflection technology for directional long drilling in ZhaoGu No.2 mine," *EnviroPro Energy*, vol. 42, pp. 13–17, 2020.

[27] H. Wang, X. Fang, F. Du et al., "Three-dimensional distribution and oxidation degree analysis of coal gangue dump fire area: a case study," *Science of The Total Environment*, vol. 772, Article ID 145606, 2021.

[28] C. Xin, F. Du, K. Wang, C. Xu, S. Huang, and J. Shen, "Damage evolution analysis and gas–solid coupling model for coal containing gas," *Geomechanics and Geophysics for Geo-Energy and Geo-Resources*, vol. 7, p. 7, 2021.

[29] Q. Wang, H. Gao, B. Jiang, S. Li, M. He, and Q. Qin, "In-situ test and bolt-grouting design evaluation method of underground engineering based on digital drilling," *International Journal of Rock Mechanics and Mining Sciences*, vol. 138, Article ID 104575, 2021.

[30] Q. Wang, Q. Qin, B. Jiang et al., "Mechanized construction of fabricated arches for large-diameter tunnels," *Automation in Construction*, vol. 124, Article ID 103583, 2021.